

On Protecting Agentic Systems' Intellectual Property via Watermarking

Liwen Wang¹, Zongjie Li¹, Yuchong Xie¹, Shuai Wang¹, Dongdong She¹, Wei Wang¹, Juergen Rahmel²

¹The Hong Kong University of Science and Technology ²HSBC

{lwanged, zligo, yxiece, shuaiw, dongdong, weiwa}@cse.ust.hk juergen.rahmel@hsbc.com.hk

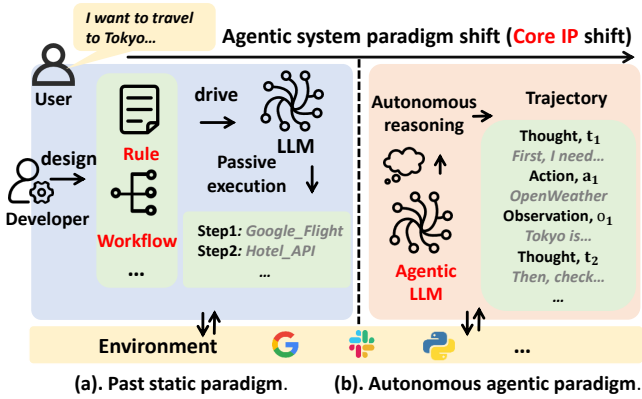


Fig. 1. The paradigm shift in agentic system architectures.

Abstract—The evolution of Large Language Models (LLMs) into agentic systems that perform autonomous reasoning and tool use has created significant intellectual property (IP) value. We demonstrate that these systems are highly vulnerable to imitation attacks, where adversaries steal proprietary capabilities by training imitation models on victim outputs. Crucially, existing LLM watermarking techniques fail in this domain because real-world agentic systems often operate as grey boxes, concealing the internal reasoning traces required for verification. This paper presents AGENTWM, the first watermarking framework designed specifically for agentic models. AGENTWM exploits the semantic equivalence of action sequences, injecting watermarks by subtly biasing the distribution of functionally identical tool execution paths. This mechanism allows AGENTWM to embed verifiable signals directly into the visible action trajectory while remaining indistinguishable to users. We develop an automated pipeline to generate robust watermark schemes and a rigorous statistical hypothesis testing procedure for verification. Extensive evaluations across three complex domains demonstrate that AGENTWM achieves high detection accuracy with negligible impact on agent performance. Our results confirm that AGENTWM effectively protects agentic IP against adaptive adversaries, who cannot remove the watermarks without severely degrading the stolen model's utility.

1 INTRODUCTION

The advent of Large Language Models (LLMs) has transcended the boundaries of text generation, giving rise to *agentic systems* [1–3]. Unlike traditional models confined to internal knowledge, these systems use a perception-action loop to interact directly

with external environments, enabling them to achieve superior performance on complex and reasoning-intensive tasks [4, 5]. By orchestrating a diverse library of tools (e.g., search engines, code interpreters), agentic systems bridge the gap between text generation and concrete execution. Given a user query, an agentic system generates a trajectory of actions (i.e., tool invocations) through continuous interaction with external environments.

As these agentic systems mature, their underlying architecture has undergone a fundamental shift. Early agentic frameworks [6–8] relied heavily on developer-crafted workflows with hardcoded execution logic, as shown in Fig. 1(a). In these systems, developers manually designed tool orchestration patterns through iterative trial and error, while LLMs served merely as passive executors within fixed pipelines [9]. This paradigm is rapidly evolving with the emergence of reasoning models such as OpenAI o3 [10] and DeepSeek-R1 [11], alongside models specifically optimized for tool use, such as MiniMax M2.1 [12]. As illustrated in Fig. 1(b), modern agentic systems empower LLMs to autonomously plan task requirements and dynamically select appropriate tools, eliminating the need for predefined workflows. This transition fundamentally redefines the nature of Intellectual Property (IP) in agentic systems: value has shifted from human-designed orchestration logic to the model's intrinsic agentic capabilities. Moreover, developing such capabilities requires substantial investment in post-training on high-quality datasets [10–12], making the agentic models themselves valuable proprietary assets that warrant protection.

Prior work demonstrates that LLMs are highly vulnerable to imitation attacks [13–16]. In these attacks, adversaries query a victim model to train a surrogate that mimics its performance [15, 16]. Although agentic systems represent an emerging field, we show that they are equally susceptible. Extracting agentic capabilities is technically feasible and proves no more challenging than extracting a standard LLM. As detailed in Sec. 3.2, our empirical analysis confirms that an extracted imitation agent (denoted as \mathcal{M}_{imi}) achieves 95% of the victim's performance. These findings expose a critical vulnerability in agentic systems, highlighting the urgent need to mitigate imitation attacks and prevent IP theft.

Detecting imitation attacks poses unique challenges. Unlike jailbreak attacks [17, 18] or adversarial inputs [19, 20] that exhibit detectable malicious patterns, imitation attacks operate through benign queries indistinguishable from legitimate user interactions. This makes runtime detection infeasible without severely degrading user experience through false positives. Consequently, recent works

propose watermarking as a robust alternative for protecting LLM IP [21–24]. These methods inject WM signals into the victim model’s outputs. When an adversary uses this data to train an imitation model \mathcal{M}_{imi} , the WM persists, serving as verifiable proof of theft. This issue extends beyond academia; protecting model IP has attracted significant industrial attention. Leading providers such as Google have deployed watermarking to secure their proprietary assets [25].

However, existing watermarking techniques cannot be directly applied to agentic systems due to their distinctive operational characteristics. Unlike traditional LLMs that expose full text outputs, agentic systems generate intermediate steps (e.g., thought-action-observation) alongside final responses. In real-world deployments, providers often conceal these intermediate steps to prevent imitation attacks, exposing only the final actions for billing purposes. We empirically validate this practice through a survey of 29 commercial agentic platforms, finding that 82.8% adopt such grey-box visibility strategies (Appendix A). This visibility constraint fundamentally undermines existing LLM watermarking techniques, which depend on access to complete textual outputs for signal injection and verification. When the majority of tokens are withheld during inference, watermark (WM) detection becomes infeasible.

This work proposes the first watermarking technique specifically designed for agentic systems. Our approach builds on a key observation: agentic execution paths contain numerous semantically equivalent action segments. For instance, a task can be accomplished using either a composite tool or multiple sub-tools in sequence. Replacing an action segment with its semantic equivalent yields functionally identical outcomes while preserving high service utility for legitimate users. Crucially, these mutations are indistinguishable from normal execution patterns, making them robust against adversarial detection. Based on this insight, we design AGENTWM, a watermarking framework where each WM corresponds to a carefully biased distribution \hat{D}_i over equivalent action segments in the agent’s output action trajectory.

We instantiate AGENTWM with five watermark schemes in two categories: *action-based* schemes exploit equivalence among individual tool calls (e.g., vendor alternatives, interface aliases), while *structure-based* schemes leverage equivalent multi-action compositions (e.g., atomic vs. decomposed operations). Based on these schemes, we develop an automated pipeline that produces a pool of verified watermark passes from the tool library. During deployment, each user receives a unique subset of passes determined by the user ID; activated passes bias matched action segments from D_i to \hat{D}_i in returned trajectories. For verification, AGENTWM employs statistical hypothesis testing to detect whether a suspicious model reproduces the watermarked distribution, providing quantifiable evidence of IP theft.

We evaluate AGENTWM across three domains (Social, Data, Business) and diverse backbone LLMs. Results show that watermarking preserves trajectory quality ($\leq 3\%$ degradation) and downstream performance (e.g., ARC: 80.09% vs. 80.43%) with only 0.28% latency overhead. AGENTWM achieves high detection ($F1 = 1.0$) and localizes malicious users with 0.92–1.0 accuracy under proper configuration. Against removal attacks, adversaries achieve $F1 < 0.02$ in identifying watermark tokens; even fully knowledgeable attackers cannot remove watermarks without severe quality loss (e.g., $\sim 36\%$ drop in trajectory quality). Perplexity [26] analysis confirms watermarked outputs are statistically indistinguishable from clean ones. Ablation studies further validate generalizability across backbone LLMs and configurations.

TABLE 1
Key notation used in the paper.

Notation	Description
$s_j = (t_j, a_j, o_j)$	The j -th intermediate step, including thought (t_j), action (a_j), and observation (o_j)
$q_i; s_i = (s_1, \dots, s_n)$	The i -th user query; sequence of intermediate steps
$r_i; \mathbf{a}_i = (a_1, \dots, a_n)$	Final response to q_i ; sequence of actions for q_i
$\tau_i = (s_i, r_i); \tilde{\tau}_i = (\mathbf{a}_i, r_i)$	Complete trajectory; grey-box trajectory
U_{id}	A random, unpredictable UID assigned to each user
$\mathcal{M}_{vic}, \mathcal{M}_{pub}, \mathcal{M}_{imi}$	Target agentic model; public backbone LLM; and attacker’s imitation agentic model
D_{ft}, D_{test}	Fine-tuning dataset split; testing dataset split
P_i, \mathcal{E}_i	Each WM pass; the equivalent action segment set in P_i
\mathcal{P}_{id}	A set of WM passes assigned to user U_{id}
D_i	Distribution of \mathcal{E}_i in D_{ft}
\hat{D}_i	Tweaked distribution (i.e., WM) of \mathcal{E}_i
θ_j, θ_N	Detection thresholds for JSD and number of detected passes

Contributions.

We summarize our contributions:

- 1) We formulate the IP protection problem for agentic systems under realistic grey-box constraints and present AGENTWM, the first watermarking framework designed for this setting.
- 2) We propose a distribution-level watermarking approach that exploits semantic equivalence in action sequences. We design five complementary schemes, an automated pipeline to instantiate watermark passes at scale, and a statistical verification procedure for provable IP theft detection.
- 3) We evaluate AGENTWM across three domains, showing that it preserves trajectory quality ($\leq 3\%$ degradation) with 0.28% latency overhead, achieves high detection ($F1 = 1.0$), and resists both partially and fully knowledgeable adversaries.

2 PRELIMINARIES AND RELATED WORKS

2.1 Preliminaries

Agentic Systems. LLMs’ capabilities in natural language understanding and generation underpin modern agentic systems [1–3], which tackle complex tasks through multi-turn interactions with external environments. As shown in Fig. 1(a), early implementations relied on developer-crafted workflows with hardcoded logic, where LLMs served as passive executors within fixed pipelines, limiting flexibility and generalization. The emergence of reasoning LLMs (e.g., OpenAI o3 [10], DeepSeek-R1 [11]) has shifted this paradigm (Fig. 1(b)): instead of following predefined patterns, modern LLMs autonomously reason and interact with their environment based on the query and context. Formally, an agentic system processes a user query q to produce a response r through intermediate steps $s_j = (t_j, a_j, o_j)$, where each step comprises a thought (t_j), an action (a_j), and an observation (o_j), forming a trajectory $\tau = (\mathbf{s}, \mathbf{r})$ with $\mathbf{s} = (s_1, \dots, s_n)$. Table 1 summarizes the key notation used throughout this paper.

Building such autonomous capabilities requires intensive training via supervised fine-tuning (SFT) [27, 28] and reinforcement learning (RL) [29, 30] on curated datasets [31, 32]. This shifts the locus of IP from explicit, human-defined logic to the internalized reasoning patterns embedded within agentic models. To deliver these capabilities, platforms like Coze [33] and Dify [34] offer *domain-specific* agentic services. However, this creates a transparency-security dilemma: platforms must disclose tool usage for billing, yet revealing the full trajectory τ exposes IP to adversaries [35–37]. To balance both concerns, platforms adopt a *grey-box* visibility setting (Sec. 3.1), revealing only the action sequence \mathbf{a} while concealing internal reasoning t_j and observations o_j . Our survey of 29 commercial agentic platforms (e.g., Coze [33],

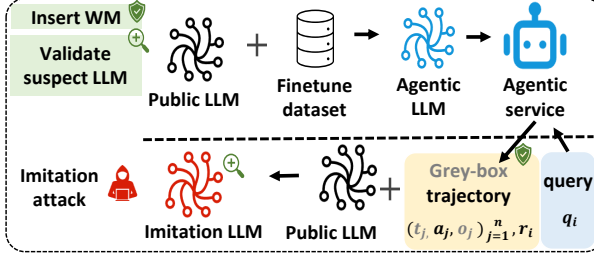


Fig. 2. Overview of the imitation attack and mitigation enabled by AGENTWM.

Dify [34]) confirms that 24 (82.8%) enforce this grey-box strategy. Details are in Appendix A.

Trajectory Equivalence. A key property of agentic models is *trajectory equivalence*: given the same query q , an agent can produce different trajectories τ_1, τ_2, \dots that lead to functionally identical final responses [38–41]. This stems from the agentic model’s inherent decision flexibility: at each step, multiple valid actions (e.g., different tools or reasoning paths) may satisfy the same intermediate goal, and these choices cascade into distinct yet functionally equivalent trajectories [38–40]. This phenomenon creates a trajectory space for each query q , containing multiple valid execution paths. This trajectory diversity enables watermarking: a defender can steer the agentic model toward specific trajectories as watermark signals, while maintaining response quality.

Imitation Attack. An imitation attack (also known as model extraction or model stealing) aims to replicate the behavior of a target model \mathcal{M}_{vic} [13–16, 42]. The adversary builds a local imitation model \mathcal{M}_{imi} to bypass service fees or offer competing services. To launch such an attack, the adversary repeatedly interacts with the victim’s domain-specific agentic model. As shown in Fig. 2, the attacker first prepares a query set Q based on domain-specific knowledge provided by the platform. For each query q_i , the victim model returns a trajectory τ_i (or $\tilde{\tau}_i$ under grey-box visibility). The attacker then fine-tunes the same public backbone LLM \mathcal{M}_{pub} using the collected dataset $\{(q_i, \tau_i)\}_{i=1}^m$ to produce \mathcal{M}_{imi} . Such attacks have proven effective across various domains, including diffusion models [42] and LLMs [13–16]. In many cases, \mathcal{M}_{imi} achieves performance comparable to or even better than \mathcal{M}_{vic} , enabling the adversary to replicate the victim’s intellectual property at minimal cost [13–16, 42].

2.2 Existing WM Techniques

Existing LLM watermarking techniques fall into two primary categories.

Content Watermarking. These methods embed watermark signals into token generation patterns. Early work such as KGW [43] partitions the vocabulary into “red” and “green” lists, biasing token selection toward green tokens. Building on KGW, subsequent efforts have introduced several improvements. For example, entropy-based sampling [44] reduces the impact on text fluency. SIR [45] and Semstamp [46] incorporate semantic information into watermark generation, ensuring that similar semantic content maps to consistent watermark patterns for improved robustness. Gumbel-Softmax watermarking [47] optimizes the biasing strategy to provably minimize degradation in text quality. CoTGuard [48] embeds watermark patterns in the model’s CoT reasoning and verifies watermarks by checking consistency between Chain of Thought (CoT) content and final responses. Additionally, agent

watermarking remains largely underexplored. The only prior work [49] targets a limited setting where the LLM outputs action probability values as text, and was evaluated on a small action space of six actions in single-step tasks. However, real-world agents typically derive actions from logits and handle multi-step tasks, limiting the applicability of this approach to practical deployments.

Model Watermarking. These approaches embed watermark signals directly into model parameters. One line of work relies on white-box verification, where specific parameter characteristics serve as identifying fingerprints. For instance, [50] extracts statistical properties from model parameters, while EaaW [51] embeds multi-bit watermarks into feature attribution explanations. Another line leverages backdoor-based mechanisms, where the model produces predefined responses when triggered by specific inputs. For example, Instructional Fingerprinting [52] uses instruction-following tasks to elicit deterministic signatures under black-box queries.

Comparison and Limitations. As shown in Table 2, existing watermarking techniques face significant limitations when applied to agentic systems. Text watermarking fails under grey-box constraints: agentic models produce concise final responses with insufficient tokens for reliable detection, and watermarking tool calls (e.g., `code_interpreter`) corrupts their strict syntax, breaking functionality. Model parameter watermarking requires white-box access for verification, which is impossible when attackers deploy black-box imitation models. Backdoor-based methods suffer from two critical flaws: backdoor signatures are easily disrupted during fine-tuning [52], and they cannot provide user-level traceability at scale. The only prior agent watermarking work [49] addresses a limited scenario with text-based action probabilities and single-step tasks, leaving multi-step agentic workflows unaddressed. These gaps collectively motivate AGENTWM: a watermarking framework designed specifically for the grey-box, multi-step nature of agentic systems.

3 MOTIVATION

3.1 Threat Model

Target Agentic Systems. We focus on commercially deployed domain-specific agentic systems on platforms such as Dify [34]. As discussed in Sec. 2, we consider the grey-box visibility model commonly adopted by commercial agentic platforms. This model balances IP protection with operational transparency by concealing internal reasoning steps while disclosing two essential components: (1) the action sequence $\mathbf{a} = (a_1, \dots, a_n)$, which documents tool usage for billing purposes, and (2) the final response r , which constitutes the delivered service output. These components form the grey-box trajectory visible to users. While some platforms optionally expose partial reasoning or intermediate tool parameters, such information is often summarized, filtered, or inconsistently provided, rendering it unsuitable as a reliable detection signal. Our grey-box model therefore captures the minimal yet reliably available information across real-world deployments.

Following standard practices in the literature, we assume that neither the service provider nor potential attackers train foundation models from scratch. Instead, both parties build upon publicly available backbone LLMs, denoted as \mathcal{M}_{pub} . The service provider fine-tunes \mathcal{M}_{pub} on a private dataset D_{ft} containing high-quality domain-specific trajectory data, producing the victim model \mathcal{M}_{vic} (e.g., a specialized travel planner or financial advisor).

TABLE 2

Comparison of AGENTWM with existing watermarking techniques. **PF**: Parameter-Free (no access to model parameters required); **GB**: Grey-Box compatible (operates when only action sequences are visible); **AS**: Agent-Supported; **FH**: Functionally Harmless (preserves tool call correctness); **DA**: Domain-Agnostic (generalizes across diverse agentic domains); **UT**: User-level Traceability at scale.

Method	PF	GB	AS	FH	DA	UT
KGW [43]	✓	✗	✗	✗	✓	✗
EaaW [51]	✗	✓	✓	✓	✓	✓
IF [52]	✗	✓	✓	✗	✓	✗
[49]	✓	✓	✓	✗	✗	✗
AGENTWM (Ours)	✓	✓	✓	✓	✓	✓

Notably, we do not assume that the victim and attacker necessarily use identical backbone models. While prior work on LLM fingerprinting demonstrates that identifying the backbone model is highly feasible, our framework aims for broader applicability. In our main experiments, we adopt the conservative assumption that both parties use the same \mathcal{M}_{pub} to establish a clear baseline. We then evaluate cross-model generalization in Sec. 7.5, where we analyze scenarios involving different backbone models to demonstrate the robustness of our approach.

Adversary Capabilities and Goals. We assume an adversary capable of querying the target agentic API within a reasonable budget to facilitate model extraction. As illustrated in Fig. 2, the adversary’s primary objective is to replicate the proprietary capabilities of the victim model. To achieve this, the attacker first harvests a collection of grey-box trajectories $\tilde{\tau}$ through extensive querying. We posit a sophisticated adversary who employs advanced reconstruction techniques to infer the concealed reasoning steps or extract intermediate content, leveraging methods such as auxiliary LLM prompting [53] or prompt stealing [36, 54]. This assumption represents an upper-bound threat model, where the adversary successfully reconstructs the grey-box observations into complete trajectories τ . Subsequently, the attacker fine-tunes their imitation model \mathcal{M}_{imi} on these reconstructed trajectories to clone the victim’s behavior.

For clarity, we detail the specific assumptions regarding IP theft detection in Sec. 5. Note that while prior research has investigated the leakage of private training data from LLMs [55], such work focuses on privacy violations rather than behavioral cloning. Therefore, those findings are distinct from and orthogonal to the intellectual property protection focus of this paper.

3.2 Imitation Attacks Demo

Setup. Imitation attacks on LLMs and diffusion models have become a well-documented threat [13–16, 42]. To motivate our watermark-based protection, we conduct a proof-of-concept (PoC) attack on a representative agentic model. We start with Qwen3-4B [56], a popular open-source LLM, and fine-tune it on our domain-specific dataset D_{ft} to create the victim agentic model \mathcal{M}_{vic} . We introduce D_{ft} and evaluation metrics in Sec. 6. For the attack, we query \mathcal{M}_{vic} to collect grey-box trajectories $\tilde{\tau}$ and reconstruct them into complete trajectories τ using an auxiliary LLM, following the standard imitation attack setup described in Sec. 2. We then fine-tune another instance of Qwen3-4B on these reconstructed trajectories to obtain the imitation model \mathcal{M}_{imi} .

Attack Results. Table 3 presents the effectiveness of the imitation attack. We evaluate model performance using three complementary

TABLE 3

Performance comparison between victim model, baseline model, and imitation model. PR: Pass Rate, RS: Response Score, TS: Trajectory Score. All metrics are higher is better.

Model	PR	RS	TS
\mathcal{M}_{vic}	0.687	0.574	0.903
\mathcal{M}_{pub} (No imitation)	0.418	0.339	0.596
\mathcal{M}_{imi} (with imitation)	0.652	0.547	0.834

metrics (detailed in Sec. 6). The results demonstrate the threat posed by imitation attacks. Without imitation, the baseline model \mathcal{M}_{pub} achieves only about 60% of the victim’s performance. However, after fine-tuning on stolen trajectories, the imitation model \mathcal{M}_{imi} achieves performance comparable to that of the victim model.

Our results in Table 3 serve as a proof-of-concept to demonstrate the feasibility of imitation attacks on agentic models. In practice, real-world attackers often employ advanced techniques [16, 57] to achieve comparable model performance with significantly fewer queries. This further amplifies the threat posed by imitation attacks. While our PoC establishes the viability of such attacks, we note that not all agentic models are equally vulnerable. Some commercial systems (e.g., Manus [58]) completely hide their internal execution details and may employ additional defenses, making imitation substantially harder. Nevertheless, our results confirm that imitation attacks pose a realistic and serious threat to many deployed agentic models, motivating the need for effective watermarking protection.

3.3 Design Considerations

Given the unique challenges of watermarking agentic models under grey-box constraints, we identify five key properties that an effective watermarking solution must satisfy. These considerations guide our design and evaluation of AGENTWM.

Fidelity. Watermarking must preserve the agentic model’s utility across multiple dimensions. First, final response quality must remain unchanged to ensure consistent user experience. Second, action sequences must maintain both semantic quality and functional equivalence, as any degradation in executable logic or API compatibility directly impacts task success rates. Third, the model’s performance on general domains must be preserved to ensure watermarking does not compromise broader capabilities beyond the protected domain.

Reliability. The watermark verification process must achieve high true positive rates when detecting imitation models while maintaining low false positive rates on unrelated models. This ensures reliable IP verification without false accusations. Additionally, the watermark must provide traceability to identify specific malicious users who access the victim model, enabling effective accountability for IP theft.

Robustness. Watermarks must persist against adversarial removal attempts. Attackers may deploy various strategies to eliminate watermark signals from stolen trajectories, such as randomly deleting tokens, using LLMs to rephrase trajectories, or replacing suspected watermarked elements. The watermark should survive these removal attacks without requiring the victim model owner to predict specific attack strategies in advance.

Stealthiness. Watermarked trajectories should be indistinguishable from normal trajectories to prevent detection and filtering during data collection. If attackers can identify watermarked samples,

they can discard them before training imitation models, rendering the watermark ineffective. This requires the watermark to blend naturally with typical behavior patterns.

Cost. Both watermark insertion and verification should incur minimal computational overhead. The insertion process should not significantly increase inference latency or deployment costs. Verification should be efficient enough to enable practical IP enforcement without excessive queries or computational resources, ensuring real-world feasibility.

We design AGENTWM to satisfy all five considerations. We introduce the technical details of AGENTWM in the following section and systematically evaluate each property in Sec. 7.

4 METHODOLOGY

Our approach is founded on the key observation that multiple equivalent intermediate steps can achieve the same outcome within the agent’s trajectory space, as discussed in Sec. 2. These sequences may differ syntactically yet preserve functional semantics. We exploit this multi-path property to embed watermarks. However, the grey-box visibility constraint (Sec. 3.1) restricts what users can observe. Embedding watermarks in concealed intermediate reasoning steps would render them unverifiable during IP theft detection. We therefore focus exclusively on the action sequence \mathbf{a} , which remains consistently visible in the grey-box trajectory $\tilde{\tau} = (\mathbf{a}, r)$.

Specifically, when a potentially malicious user submits a query, the agent first generates a raw trajectory τ . Before returning the grey-box trajectory $\tilde{\tau} = (\mathbf{a}, r)$ to the user, AGENTWM intercepts the output and applies a series of watermark passes. The watermark passes transform the original \mathbf{a} into a watermarked version \mathbf{a}_{wm} by injecting subtle, user-specific patterns while strictly preserving functional semantics. AGENTWM then returns $\tilde{\tau}_{wm} = (\mathbf{a}_{wm}, r)$, thereby embedding provenance signals without compromising service utility.

4.1 WM Definition

We formalize watermarks as induced distribution shifts over the space of equivalent action sequences.

Definition 1 (Watermark). An action sequence watermark exploits the fact that equivalent action sequences can produce nearly identical final responses despite their syntactic differences. Formally, a watermark pass P_i is defined by an equivalent action segment set $\mathcal{E}_i = \{w_1, w_2, \dots, w_k\}$. This set contains distinct action segments (i.e., sub-sequences of actions) that perform an identical semantic function. Let D_i denote the natural probability distribution of these segments in the Dft. The watermark P_i transforms an action sequence \mathbf{a} into \mathbf{a}' by detecting any segment $w \in \mathcal{E}_i$ and replacing it with a substitute $w' \in \mathcal{E}_i$ sampled from a biased target distribution \hat{D}_i . This replacement embeds a statistical signature while preserving the functional utility of \mathbf{a} .

We design five distinct watermarking schemes that exploit equivalence from complementary perspectives (Sec. 4.3). To instantiate these schemes at scale, we develop an automated pipeline (Sec. 4.4) to mine equivalence patterns, generating hundreds of unique watermark passes.

4.2 WM Insertion Procedure

Fig. 3 illustrates the watermark insertion phase in AGENTWM. We detail the three key steps below. The verification phase (IP theft check) is discussed in Sec. 5.

① Deriving Target Distribution \hat{D}_i . For each watermark pass P_i corresponding to an equivalence set $\mathcal{E}_i = \{w_1, w_2, \dots, w_k\}$, we construct a target distribution \hat{D}_i . Let $p(w_j)$ denote the natural probability of segment w_j in the victim agent’s original distribution D_i . Following standard watermarking principles [21], we apply a logit bias to shift D_i toward \hat{D}_i . Specifically, we strictly designate one segment $w_t \in \mathcal{E}_i$ as the *target segment* and boost its probability via exponential scaling. The target probability $\hat{p}(w_j)$ is computed as:

$$\hat{p}(w_j) = \begin{cases} \frac{p(w_t) \cdot e^\delta}{p(w_t) \cdot e^\delta + \sum_{k \neq t} p(w_k)} & \text{if } w_j = w_t \\ \frac{p(w_j)}{p(w_t) \cdot e^\delta + \sum_{k \neq t} p(w_k)} & \text{otherwise} \end{cases} \quad (1)$$

where δ is a hyperparameter controlling the bias strength. This operation creates a statistically detectable shift toward w_t while maintaining a valid probability distribution. We also discuss the impact of δ in Sec. 7.5.

② User Registration and Pass Assignment. Upon registration, each user is assigned a unique N -bit User ID (UID) U_{id} , where N is the total number of available watermark passes. We require U_{id} to be random, unique, and cryptographically unpredictable to attackers.¹ The U_{id} determines the specific subset of watermark passes \mathcal{P}_{id} activated for that user. The mapping $\mathcal{P}_{id} \leftarrow U_{id}$ activates pass P_{i+1} if and only if the i -th bit of U_{id} is 1 (for $i \in [0, N-1]$).

Since \mathcal{P}_{id} is unique to each user, it acts as a digital fingerprint for identifying malicious users involved in IP theft (see Sec. 5). To balance detection reliability with user capacity, we constrain the Hamming weight of the UID (i.e., the number of active passes $|\mathcal{P}_{id}|$) to the range [5, 20]. Even in the only one domain (Data, $N = 39$ passes; see Table 4), this already yields approximately 343 billion unique UIDs,² far exceeding the user base of any real-world platform. Domains with more passes provide even greater capacity. Activating too few passes reduces verification confidence (Sec. 7.2), while activating too many increases the collision probability between users, hindering precise attribution.

③ Applying Watermark Passes. During inference, when the agent generates a trajectory for a user with pass set \mathcal{P}_{id} , AGENTWM intercepts the visible action sequence \mathbf{a} . It scans \mathbf{a} to identify any subsequences that match the equivalence sets \mathcal{E}_i of the currently active passes in \mathcal{P}_{id} . For each identified match, AGENTWM samples a replacement segment from the corresponding target distribution \hat{D}_i and substitutes it in place. The modified trajectory is then returned to the user.

4.3 WM Scheme Taxonomy

Each watermark scheme defines a class of equivalence groups over action segments. Recall that a watermark pass biases the distribution over an equivalence set \mathcal{E}_i (Sec. 4.1); the schemes differ in *how equivalence is defined*. Analogous to instruction-level vs. block-level transformations in program analysis, we organize schemes into two categories (Fig. 4). *Action-based* schemes define equivalence over individual tool calls: each member of \mathcal{E}_i is a single invocation. *Structure-based* schemes define equivalence over multi-action sub-sequences: each member is an ordered sequence of calls that jointly achieve the same outcome. This orthogonal design expands the combinatorial space an adversary must search to remove watermarks (Sec. 7.3). All schemes preserve task semantics

1. This can be implemented using salted cryptographic hash functions (e.g., SHA-256) [59].

2. $\sum_{k=5}^{20} \binom{39}{k} \approx 343$ billion for $N = 39$.

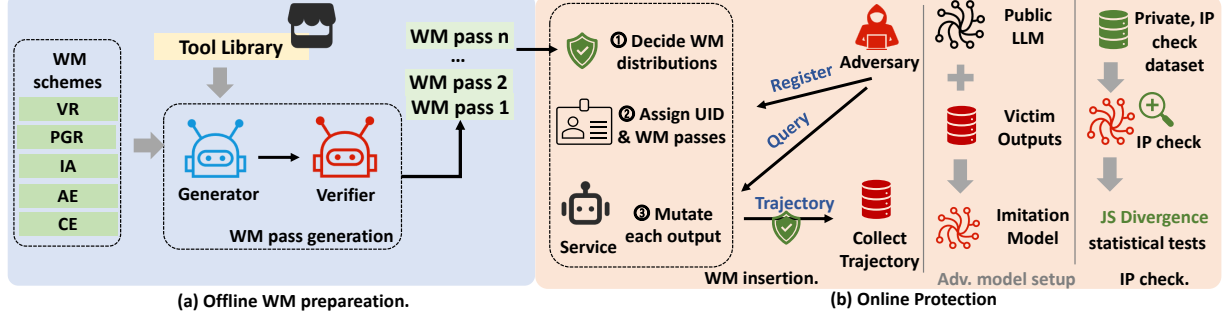


Fig. 3. Overview of AGENTWM. (a) Offline watermark preparation: the Generator mines candidate equivalence sets from the tool library with five WM schemes, and the Verifier validates them to produce watermark passes. (b) Online protection: AGENTWM assigns user-specific passes, applies watermarks to trajectories, and detects IP theft through statistical divergence tests.

and incur negligible overhead. Table 4 summarizes the distribution of passes across schemes and domains.

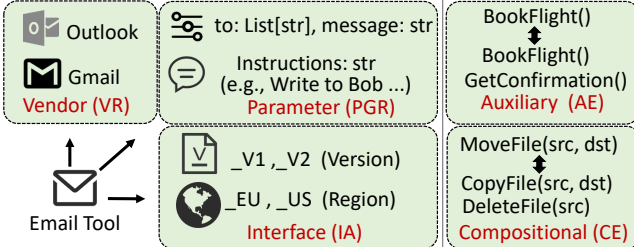


Fig. 4. Taxonomy of five watermark schemes. Each defines a distinct class of equivalence groups over action segments, enabling distribution-level watermark embedding.

Action-Based Schemes. Real-world tool ecosystems exhibit pervasive functional redundancy: multiple tools perform identical operations yet differ in provider, interface, or parameterization. We identify three orthogonal sources of such redundancy, each defining a distinct class of equivalence groups.

Vendor Replacement (VR). Common functionalities (e.g., email, translation, weather queries) are served by competing providers. VR groups tools that provide identical functionality from different vendors into equivalence set. For instance, $\{w_1 = \text{Outlook}.\text{SendEmail}, w_2 = \text{Gmail}.\text{SendEmail}\}$: both expose identical semantics, and the vendor choice carries no functional significance. Such groups arise naturally from ecosystem redundancy, making the distributional bias inherently stealthy.

Parameter Granularity Replacement (PGR). Functionally equivalent tools may expose parameters at different abstraction levels. PGR groups tools that accept coarser or finer-grained inputs for the same operation. For example, one email tool takes structured fields (to, subject, body), while another accepts a single natural-language instruction (e.g., "Write to Bob..."). Both produce the same result. PGR places them in equivalence set; the interface granularity defines the equivalence.

Interface Aliasing (IA). Providers often maintain multiple endpoint names for the same backend (e.g., versioned (_V1 vs. _V2) or region-specific (_EU vs. _US)). IA groups these co-referencing names into equivalence set. The alias choice carries zero semantic information yet produces a detectable distributional signature. Since aliasing arises from routine API evolution, it blends seamlessly into normal trajectories.

Structure-Based Schemes. Beyond individual calls, functional equivalence extends to how actions are *composed*. Structure-based

schemes define equivalence over multi-action sub-sequences that achieve identical outcomes through different arrangements.

Auxiliary Equivalence (AE). Agentic models routinely perform ancillary operations alongside primary actions, such as retrieving confirmation details or recording metadata. AE defines equivalence between a base sub-sequence and its variant that includes such ancillary calls. For example, $[\text{BookFlight}(\text{route}, \text{date})]$ and $[\text{BookFlight}(\text{route}, \text{date}), \text{GetConfirmation}(\text{id})]$ form an equivalence group: the flight is booked in both cases, and the confirmation query merely retrieves an already-assigned reference number without affecting the reservation. Since agents naturally exhibit both patterns, the distributional bias remains stealthy.

Compositional Equivalence (CE). Many operations admit both atomic and decomposed expressions in tool ecosystems. CE groups these equivalent representations. For instance, $[\text{MoveFile}(\text{src}, \text{dst})]$ and $[\text{CopyFile}(\text{src}, \text{dst}), \text{DeleteFile}(\text{src})]$ form an equivalence group: both achieve file relocation with identical side effects. The choice between composite and decomposed forms carries no functional significance, creating a natural watermark channel.

4.4 Watermark Instance Generation

While the taxonomy in Sec. 4.3 delineates the theoretical design space for action equivalence, operationalizing these schemes requires a scalable generation mechanism. Manual curation of equivalence sets is prohibitively expensive and inherently unscalable, particularly given the rapid evolution of real-world tool ecosystems. We therefore construct an automated pipeline that systematically instantiates watermark passes for the defined schemes. Our core design principle is the *decoupling of candidate mining from equivalence validation*. This separation allows us to maximize recall during exploration of the vast tool space, while subsequently enforcing precision through rigorous verification. The pipeline operates in two phases, implemented by a **Generator** and a **Verifier** as shown in Fig. 3(a).

Phase 1: Candidate Mining (Generator). Given a tool library \mathcal{T} and a target watermark scheme S , the goal is to identify candidate tool pairs or sequences that may exhibit equivalence under S . We use the xlam-function-calling-60k dataset [60] as our tool library \mathcal{T} , comprising 3,673 tools (detailed in Sec. 6). To manage the combinatorial explosion of pairwise comparisons, we employ a two-stage filtering strategy. First, we leverage an embedding Qwen3-

embedding model [61] to prune the search space, retaining only tool pairs whose semantic representations exceed a similarity threshold. This ensures that only functionally related tools proceed to the next stage. Second, we apply scheme-specific analysis using an LLM to assess equivalence potential. For action-based schemes, the LLM examines whether tools perform equivalent atomic operations (e.g., both compute numerical aggregation). For structure-based schemes, it analyzes whether tool compositions yield equivalent execution patterns (e.g., sequential API calls with identical side effects). This process yields approximately 207 candidate equivalence pairs. This phase prioritizes recall: we deliberately cast a wide net to capture all plausible equivalence relationships, accepting false positives for subsequent refinement in Phase 2.

Phase 2: Equivalence Validation (Verifier). Phase 1 prioritizes recall over precision, producing candidates that require rigorous verification. We employ a dual-validation pipeline to eliminate false positives. First, we invoke a separate LLM to perform semantic analysis, checking whether the candidate pairs preserve identical functional behavior under representative inputs. Second, we execute both candidate pairs in our sandboxed environment (Sec. 6) with diverse test cases, comparing outputs and side effects. Only candidates that pass both semantic and execution validation are accepted. Each validated equivalence set \mathcal{E}_i is registered as an operational watermark pass, expanding the global pool of 101 passes in Sec. 4.2. This automated pipeline produces hundreds of verified watermark instances with minimal manual effort. The first two authors further conduct post-hoc human inspection on a random sample of 50 validated instances (half of the total) and observe no functional inconsistencies, confirming the reliability of our automated validation pipeline.

5 IP THEFT VERIFICATION STAGE

In this section, we detail the verification framework used to identify IP theft. The procedure moves from individual WM detection to holistic model classification and, finally, attacker localization.

5.1 Motivation and Assumptions

Motivation. The owner of the victim model \mathcal{M}_{vic} seeks to verify whether a suspect model \mathcal{M}_{imi} was trained on its watermarked outputs. As illustrated in Fig. 3, this verification exploits the principle that imitation learning preserves the statistical biases injected by AGENTWM into the action trajectories. If \mathcal{M}_{imi} was fine-tuned on watermarked trajectories, it will exhibit the same distributional patterns embedded during watermark injection.

Assumptions. Following the threat model defined in Sec. 3.1, the adversary leverages grey-box trajectories to fine-tune a public backbone \mathcal{M}_{pub} . Each registered user receives a unique identifier (UID) U_{id} mapped to a distinct WM pass set \mathcal{P}_{id} , enabling attribution of theft to specific malicious users. Regarding watermark knowledge, we consider two levels of adversary awareness. A

Partially Knowledgeable (PK) Attacker is aware of the watermark’s existence but lacks knowledge of the specific watermarking schemes employed by AGENTWM. A **Fully Knowledgeable (FK) Attacker** knows all five candidate watermarking schemes but cannot determine the exact WM pass set \mathcal{P}_{id} assigned to the target service. Each watermarking scheme involves numerous configurable parameters (such as which actions to transform, the specific transformation rules, and watermark strength), and the space of possible configurations grows exponentially. Consequently, even with full knowledge of the schemes, the FK attacker faces

substantial uncertainty in identifying or removing the precise watermark configuration.

For verification, the owner uses a private dataset \mathcal{V}_{v} to query \mathcal{M}_{imi} . Following standard assumptions in prior watermarking literature [21], we assume \mathcal{V}_{v} is not publicly accessible and shares the same distribution as the original fine-tuning data D_{ft} used to train \mathcal{M}_{vic} .

5.2 Verification Procedure

Detection of Individual WM Passes. To check for a specific WM pass P_i , we query the suspect model \mathcal{M}_{imi} with the private verification dataset \mathcal{V}_{v} and collect its grey-box trajectories. From these trajectories, we compute the empirical distribution D'_i of equivalent action segment sets. We then quantify the discrepancy between D'_i and the target distribution \hat{D}_i embedded during watermark injection using Jensen-Shannon Divergence (JSD). As a symmetric metric bounded in $[0, 1]$, a lower JSD value signifies greater distributional similarity. A pass P_i is considered detected if $\text{JSD}(D'_i, \hat{D}_i) < \theta_j$, where θ_j is the sensitivity threshold. A JSD value below θ_j provides strong evidence that the training data of \mathcal{M}_{imi} contains the watermark pattern from pass P_i .

Holistic Model Classification. Since the identity of the model’s trainer is initially unknown during verification, we test \mathcal{M}_{imi} against the global pool of all N WM passes in AGENTWM. For each pass P_i , we mark it as detected if its JSD value falls below θ_j . Let n_{det} denote the total count of detected passes. The suspect model \mathcal{M}_{imi} is classified as an imitation model only if $n_{\text{det}} \geq \theta_N$, where θ_N is the detection threshold. This two-level thresholding design balances robustness and accuracy: θ_j controls per-pass sensitivity to reduce noise, while θ_N requires multiple passes to confirm theft, thereby minimizing false positives. We evaluate the impact of these thresholds on verification accuracy in Sec. 7.2. Most WM passes operate independently, ensuring that one watermark does not interfere with another. However, a few passes may affect the transformable candidates of subsequent passes. To ensure consistency, we apply these interdependent passes in a fixed order during both injection and verification, as defined in Sec. 4.2.

Localization of the Malicious User. Once theft is confirmed, AGENTWM identifies the specific attacker by exploiting the unique mapping between UIDs and pass sets established during user registration (Sec. 4.2). We compare the binary vector of detected passes in \mathcal{M}_{imi} against the registry of all assigned WM pass sets. To account for potential signal loss during imitation learning and data sampling variance, we employ similarity-based matching (e.g., cosine similarity) rather than requiring exact matches. A malicious user is identified when their assigned WM pass set exhibits the highest similarity to the detected passes in \mathcal{M}_{imi} . We evaluate the accuracy and robustness of this localization procedure in Sec. 7.2, including scenarios where one or two WM passes fail detection due to imitation learning quality or statistical noise.

6 IMPLEMENTATION AND SETUP

We now present the experimental setup. All experiments are performed with four NVIDIA H800 graphics cards.

Dataset. We build upon xlam-function-calling-60k [60], which contains 60,000 trajectories covering 3,673 tools across 21 domains. Since the original dataset contains limited multi-step trajectories, following the original methodology, we extend it and validate the correctness of each generated trajectory using GPT-5 [62] and DeepSeek-v3.2 [63]. We select three high-impact domains

TABLE 4
Distribution of watermark passes across five schemes and three domains.

Scheme	Domain			Total
	Data	Business	Social	
Vendor Replacement (VR)	8	12	18	38
Parameter Granularity Replacement (PGR)	7	4	2	13
Interface Aliasing (IA)	11	5	6	22
Auxiliary Equivalence (AE)	7	5	3	15
Compositional Equivalence (CE)	6	2	5	13
Total	39	28	34	101

(i.e., Social, Business, and Data) based on their prevalence in real-world agentic platforms [33, 34] and prior work [64]. The curated dataset comprises 30,000 trajectories in total. We split them into a fine-tuning set D_{ft} (24,000 samples) and a held-out test set D_{test} (6,000 samples), following standard watermarking protocols [21]. We use D_{ft} to simulate the attack, representing an upper-bound threat where adversaries possess a diverse query set. Although real attackers often bootstrap from seed queries [16], this setting provides a conservative evaluation of watermark robustness. We evaluate \mathcal{M}_{imi} on D_{test} and use D_{test} as the verification set for IP theft detection, consistent with prior work [21].

Metrics. Following standard evaluation protocols for agentic systems [65–67], we assess model performance at both task and trajectory levels. For final response quality, we measure *Pass Rate* (PR) and *Response Score* (RS). PR is a binary metric determining if the response fulfills the user request, while RS evaluates semantic quality on a 1–5 scale. For trajectory quality, we adopt *Trajectory Score* (TS) [66, 67], which evaluates the correctness and coherence of the reasoning chain on a 1–5 scale. All three metrics are scored by DeepSeek-v3.2 acting as a judge. To enable fair comparison, we normalize all scores to the [0, 1] range. We also measure downstream capabilities on ARC [68] for reasoning and ACPBench [69] for planning. For watermark reliability, we measure Precision, Recall, and F1-score for detection, and Top-1 Accuracy for malicious user localization [21]. To assess stealth, we measure perplexity (PPL) [26], which quantifies how much the watermark shifts output distribution from its natural behavior.

Model & Agentic System. We employ Qwen3-4B [56] as the base public backbone \mathcal{M}_{pub} in our main experiments, a widely adopted choice in recent agentic research [70]. We further evaluate generalization on Qwen3-8B [56] and Minstral-8B [71] in Sec. 7.5. For the agentic framework, we adopt ReAct [3]. Following [65], we use Qwen3-Next-80B-A3B [72] as the environment simulator to execute tools and generate observations. We fine-tune all models using LoRA [73] with rank $r = 64$, alpha $\alpha = 128$, and a learning rate of $2e - 4$.

Watermark Configuration. We instantiate a total of 101 watermark passes across 5 schemes (Sec. 4.3), with N ranging from 28 to 39 per domain (see Table 4). Within each domain, each user is assigned a unique N -bit User ID (U_{id}), where the i -th bit corresponds to the activation of the i -th watermark pass. For each user, we randomly activate a subset of passes (5–20) to ensure high user capacity while preserving utility.

TABLE 5
Fidelity metrics (PR, RS, TS) of victim and imitated models across different domains.

Domain	Metric	Data			Business			Social		
		PR	RS	TS	PR	RS	TS	PR	RS	TS
\mathcal{M}_{vic}		0.792	0.630	0.896	0.687	0.574	0.903	0.707	0.582	0.943
\mathcal{M}_{imi}	5–10 WM passes	0.755	0.575	0.837	0.642	0.543	0.841	0.678	0.529	0.871
	10–15 WM passes	0.703	0.591	0.860	0.637	0.537	0.858	0.663	0.536	0.868
	15–20 WM passes	0.741	0.586	0.841	0.664	0.553	0.834	0.626	0.539	0.884

7 EVALUATION

To assess whether AGENTWM meets the design properties outlined in Sec. 3.3, we organize the evaluation around five research questions (RQs):

RQ1: Fidelity & Cost. Does watermark injection degrade the functional quality of protected agentic systems? How much computational overhead does AGENTWM introduce during inference?

RQ2: Reliability. How accurately can AGENTWM identify the source of IP theft when performing verification on a suspect agentic system?

RQ3: Robustness. Can AGENTWM’s watermarks withstand removal attacks that attempt to erase embedded signatures?

RQ4: Stealthiness. Are watermarked outputs distinguishable from clean outputs to human observers or automated detectors?

RQ5: Ablation Study. How does AGENTWM generalize across different backbone LLMs, watermark strengths, and cross-model attack scenarios?

7.1 RQ1: Fidelity & Cost

We evaluate whether watermark injection degrades model quality for both legitimate users and adversaries. Given the grey-box visibility constraint (Sec. 3.1), we assess trajectory fidelity indirectly by measuring \mathcal{M}_{imi} ’s performance: if watermarks corrupt trajectories, models trained on them would exhibit severe degradation [21]. We evaluate three aspects: (1) trajectory quality (PR, RS, TS) on domain-specific tasks, (2) downstream capabilities (ARC, ACPBench) to verify general abilities remain intact, and (3) computational overhead during inference. For \mathcal{M}_{imi} , we test three watermark intensities: 5–10, 10–15, and 15–20 passes.

Final Response and Trajectory Quality. We find that watermark injection preserves both victim and imitation model quality. As shown in Table 5, \mathcal{M}_{imi} trained on watermarked trajectories maintains comparable performance to \mathcal{M}_{vic} across all domains. For instance, in the Data domain, \mathcal{M}_{imi} achieves PR of 0.703–0.755 compared to \mathcal{M}_{vic} ’s 0.792. This demonstrates two critical properties. First, watermarking does not corrupt the functional quality of trajectories, as \mathcal{M}_{imi} successfully learns domain capabilities from them. Second, the consistent performance across varying watermark intensities (5–10, 10–15, 15–20 passes) shows that AGENTWM achieves a practical balance: strong enough watermarks for reliable verification (Sec. 7.2) without degrading utility. The slight performance gap between \mathcal{M}_{vic} and \mathcal{M}_{imi} arises from inherent limitations in grey-box trajectory reconstruction, not from watermark corruption, confirming that watermarked trajectories remain valuable training signals for adversaries.

Downstream Performance. To rule out hidden degradation outside protected domains, we evaluate both \mathcal{M}_{vic} and \mathcal{M}_{imi} on ARC (complex reasoning) and ACPBench (agent planning). As shown in Table 6, watermarked models preserve downstream performance across all domains. For instance, in the Data domain, \mathcal{M}_{imi} achieves

TABLE 6
Downstream task performance of victim and imitated models across different domains.

Domain	Data		Business		Social		
	Downstream task	ARC	ACPBench	ARC	ACPBench	ARC	ACPBench
\mathcal{M}_{vic}		80.43%	46.69%	79.92%	59.15%	80.60%	59.62%
\mathcal{M}_{imi}	5–10 passes	79.88%	55.30%	79.71%	55.68%	79.12%	57.18%
	10–15 passes	80.09%	49.72%	79.63%	55.21%	79.29%	55.83%
	15–20 passes	81.06%	50.66%	80.01%	58.91%	78.91%	56.00%

TABLE 7
Overhead of watermark insertion over 1,000 queries.

Response Time (s)	WM Insertion Time (s)	Response Slowdown
3428	9.6	0.28%

80.09% on ARC compared to \mathcal{M}_{vic} 's 80.43%, demonstrating negligible degradation. This holds across different watermark intensities and benchmarks, confirming that AGENTWM's trajectory-level watermarking operates orthogonally to the model's general reasoning capabilities. This result addresses a critical concern: watermarking only affects trajectory selection within the protected domain, leaving the model's foundational abilities intact. Combined with our trajectory quality results (Table 5), this confirms that AGENTWM achieves complete fidelity preservation across both domain-specific and general-purpose capabilities.

Cost. Beyond fidelity, we quantify the computational overhead introduced by watermark injection. We measure the additional latency across 1,000 queries sampled from D_{test} on \mathcal{M}_{vic} . As shown in Table 7, watermark injection introduces only 9.6 seconds of overhead across all 1,000 queries, corresponding to a negligible 0.28% slowdown in total response time. This minimal overhead stems from AGENTWM's design: watermark injection occurs during trajectory generation (Sec. 4), where we only manipulate action sequences without invoking additional LLM calls or external computations. The overhead primarily consists of lightweight pass activation checks. This result demonstrates that AGENTWM achieves practical deployability: watermark protection incurs virtually no performance penalty, making it viable for production agentic systems serving real-time user queries.

7.2 RQ2: Reliability

To evaluate reliability, we assess whether AGENTWM can accurately (1) identify suspect models \mathcal{M}_{imi} trained on watermarked trajectories and (2) pinpoint the specific malicious user (UID) responsible for the attack.

Confirming a Suspect Model. As described in Sec. 5, given a suspect model \mathcal{M}_{imi} , we query it with a private verification dataset \mathcal{V}_i to determine whether \mathcal{M}_{imi} was trained on watermarked trajectories stolen from \mathcal{M}_{vic} . Following prior watermarking work [21], we use the test split of D_{test} as \mathcal{V}_i in our evaluation.

To ensure statistical reliability within a feasible computational budget (1,000 GPU hours), we fine-tuned a total of 36 imitation models across the three domains. For each domain, we leverage 12 of these models as positive samples (i.e., models trained on stolen watermarked trajectories). To evaluate false positive rates, we also prepare 12 benign models as negative samples per domain. These benign models are randomly sampled from the clean D_i and fine-tuned without any watermark injection. This setup ensures realistic evaluation of both detection accuracy and false alarm rates.

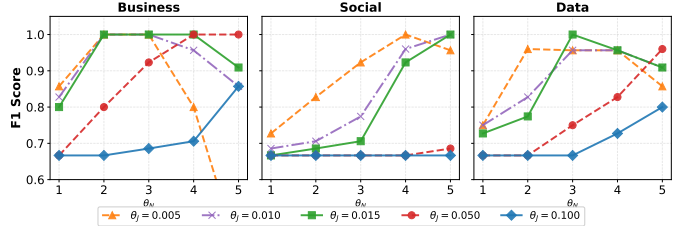


Fig. 5. Detection performance across different threshold configurations.

Our verification process (Sec. 5) relies on two hyper-parameters: θ_J (the JSD threshold for detecting individual watermark passes) and θ_N (the minimum number of detected passes required to confirm IP theft). To systematically evaluate detection accuracy, we test five JSD thresholds: $\theta_J \in \{0.005, 0.010, 0.015, 0.050, 0.100\}$. For θ_N , we consider values from 1 to 5, reflecting the fact that we inject at least 5 watermark passes per user (Sec. 7.1). We evaluate all configurations across three domains and measure performance using the F1-score: $F_1 = \frac{2PR}{P+R}$, where precision P captures the fraction of correctly identified stolen models among all flagged models, and recall R measures the fraction of stolen models successfully detected. Results are shown in Fig. 5.

Fig. 5 demonstrates that AGENTWM achieves reliable IP theft detection across diverse scenarios. With appropriate threshold configurations, AGENTWM consistently delivers high F1-scores (nearly 1.00) across all three domains, confirming its effectiveness in identifying watermarked trajectories. However, detection accuracy degrades when θ_N is improperly configured. When θ_N is too low (e.g., $\theta_N = 1$ or 2), the system becomes overly sensitive, flagging benign models that coincidentally trigger a single watermark pass. Conversely, excessively high θ_N values (e.g., $\theta_N \geq 4$) reduce detection power, as attackers may not collect enough queries to activate all embedded watermark passes. Based on our empirical analysis, we recommend setting $\theta_N = 3$ as a practical default, which balances robustness against false positives while maintaining sufficient detection sensitivity.

Localizing the Malicious User. Beyond confirming IP theft, we evaluate a harder task: pinpointing the specific malicious user from a large pool. Given 12 known malicious imitation models, we first identify each model's activated watermark passes via statistical testing. The activated passes form a binary fingerprint, represented as an N -bit vector \mathbf{v} , where N is the number of active passes in the domain. We then match \mathbf{v} against the ground-truth watermark assignments \mathbf{p}_i for all users using cosine similarity, returning the highest-similarity user as the identified adversary.

Table 8 reports results across varying pool sizes: 12 malicious users alone, and 12 malicious users mixed with 1K, 2K, 5K, and 50K randomly sampled benign users. Each experiment is repeated multiple times and we report the averaged top-1 accuracy. AGENTWM maintains high localization accuracy across all domains. Data and Business achieve 0.92–1.0 accuracy even at 50K total users. The Social domain exhibits lower accuracy (0.81 at 50K) because its tool ecosystem yields fewer distinguishing passes per trajectory, reducing fingerprint uniqueness. Overall, the accuracy degradation at extreme scales stems from increased watermark collision probability among benign users, not fundamental design limitations.

While AGENTWM theoretically supports nearly 343 billion unique identities through combinatorial watermark assignments

TABLE 8
Adversary localization accuracy under different user pool sizes with top-1 matching.

Domain	Total User Pool Size				
	12	12 + 1K	12 + 2K	12 + 5K	12 + 50K
Data	1.0	1.0	0.97	0.97	0.92
Business	1.0	1.0	1.0	0.97	0.94
Social	0.92	0.92	0.89	0.86	0.81

(5–20 passes), exhaustive search is unnecessary. Model extraction attacks require extensive querying, so investigators can filter by query volume (e.g., $> 10K$ queries), narrowing the search space from millions to a few thousand suspects.

7.3 RQ3: Robustness

Robustness measures whether AGENTWM’s watermarks survive adversarial removal attempts. The core of our defense lies in asymmetric uncertainty: while adversaries may know watermarking exists, the vast design space and flexible instantiation of our five-scheme framework make targeted removal extremely difficult. Following the threat levels defined in Sec. 5.1, we evaluate both *Partially Knowledgeable* (PK) and *Fully Knowledgeable* (FK) attackers.

PK Attackers. PK attackers operate in a black-box setting: they know watermarks exist but lack knowledge of the five schemes or their instantiation. We assume they deploy generic removal strategies adapted from text watermarking literature [23, 74]. We evaluate three representative attacks. *Random Deletion* randomly removes tokens from trajectories to disrupt embedded patterns. *LLM Rephrase* instructs an LLM to paraphrase trajectories while preserving the quality, aiming to erase watermark signals through linguistic variation. *LLM Replacement* leverages an LLM to identify and substitute potentially watermarked tokens with natural alternatives, balancing removal effectiveness and trajectory quality. We evaluate watermark attack using 1K watermarked trajectories generated by AGENTWM. For each attack strategy, we measure watermark attack accuracy via precision (fraction of detected tokens that are true watermarks), recall (fraction of true watermarks successfully detected), and F1-score (harmonic mean of precision and recall). Table 9 shows results.

Table 9 shows that all three attacks fail to remove watermarks effectively. All F1-scores remain below 0.02, indicating attackers can barely identify watermark-carrying tokens. This failure stems from a fundamental mismatch: these attacks target token-level patterns inherited from text watermarking, whereas AGENTWM embeds watermarks into action-sequence distributions at the trajectory level. Without knowledge of our five schemes or their instantiation, attackers cannot distinguish watermarked actions from natural variations in agentic reasoning. The low recall values (e.g., 0.0517 for LLM Rephrase) confirm that generic removal strategies remain blind to our distribution-level watermarks.

FK Attackers. As mentioned before, FK attackers represent the worst-case threat: they know all five watermark schemes but face a combinatorial challenge. Each scheme can generate many distinct passes (Sec. 4.3), and without knowing which specific passes were activated for a given user, attackers cannot identify watermarked action sequences in collected trajectories. This uncertainty forces them to guess which actions carry watermark signals. To evaluate

TABLE 9
Watermark detection under different attacks.

Attack Strategy	Precision	Recall	F1-Score
Random Deletion	0.0056	0.0917	0.0103
LLM Rephrase	0.0012	0.0517	0.0023
LLM Replacement	0.0020	0.1817	0.0040
FK Replacement	0.2644	0.2256	0.2350

in this worst-case scenario, we design an FK Replacement attack that exploits their scheme knowledge to optimize the baseline LLM Replacement strategy. This simulates their best effort at identifying and removing watermarked actions.

TABLE 10
Trajectory quality degradation after FK attackers attempt watermark removal. Since the final response remains unchanged, the pass rate is identical; thus we only report RS and TS.

Metric	RS	TS
Original	0.612	0.877
Watermark Removed	0.391	0.514

Results appear in the last row of Table 9. With scheme knowledge, both recall and precision improve substantially over the PK scenario. However, the F1-score (0.2350) remains low. Moreover, removal attempts severely degrade trajectory quality. As Table 10 shows, RS drops from 0.612 to 0.391 after removal, because FK attackers cannot pinpoint which passes were activated and must over-modify action sequences, disrupting the reasoning coherence. Thus, even with full scheme knowledge, attackers cannot remove AGENTWM’s watermark without rendering the stolen data unusable.

7.4 RQ4: Stealthiness

Stealthiness measures whether attackers can distinguish watermarked trajectories from clean ones. If adversaries detect watermark patterns during data collection, they can filter out watermarked samples before fine-tuning \mathcal{M}_{imi} , rendering the watermark ineffective. A stealthy watermark must preserve the statistical properties of natural trajectories, making detection infeasible without access to the victim’s private verification procedure.

Following prior work [75], we measure stealthiness using perplexity (PPL). PPL is computed by an external language model (GPT-2 [76]) to quantify text fluency, where lower values indicate more natural text. We compare the PPL of trajectories before and after watermark injection to quantify the deviation introduced by embedded watermarks.

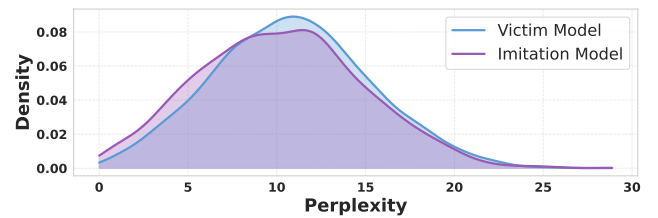


Fig. 6. PPL comparison between \mathcal{M}_{vic} and \mathcal{M}_{imi} .

Fig. 6 visualizes the PPL densities. The distributions exhibit a near-perfect overlap, with the difference in mean PPL being

TABLE 11
Performance comparison across different LLM.

Model	Fidelity			Reliability	
	PR	RS	TS	5K	50K
Minstral	\mathcal{M}_{vic}	0.702	0.582	0.904	—
	\mathcal{M}_{imi}	0.633	0.539	0.846	0.93
Qwen 8B	\mathcal{M}_{vic}	0.742	0.564	0.910	—
	\mathcal{M}_{imi}	0.678	0.581	0.878	1.0
					0.93

less than 0.5. This statistical indistinguishability confirms that AGENTWM’s distribution biasing is subtle enough to remain hidden within the inherent variance of agentic reasoning. The result validates our design principle: by manipulating action-sequence distributions rather than individual tokens, AGENTWM preserves the natural fluency of agentic reasoning. From an adversary’s perspective, watermarked trajectories remain indistinguishable from clean ones using automated perplexity-based detection. This stealthiness property is critical: it prevents attackers from filtering watermarked samples during data collection, ensuring that fine-tuning on stolen trajectories inevitably inherits embedded watermark signals. Combined with our fidelity results (Sec. 7.1), this demonstrates that AGENTWM achieves invisible protection without sacrificing utility.

7.5 RQ5: Ablation Study

Impact of Backbone LLM. We evaluate whether AGENTWM generalizes beyond Qwen3-4B by extending to Minstral-8B [71] and Qwen3-8B [56], which differ in model family and scale. We retrain both \mathcal{M}_{vic} and \mathcal{M}_{imi} from scratch for each backbone. Table 11 reports the results. AGENTWM maintains consistent performance across all backbones. Both Minstral-8B and Qwen3-8B achieve fidelity comparable to Qwen3-4B (Sec. 7.1), with only marginal degradation from \mathcal{M}_{vic} to \mathcal{M}_{imi} (e.g., PR: 0.742 \rightarrow 0.678 on Qwen3-8B). Reliability also holds: top-1 accuracy remains 0.93–1.0 under 5K–50K user pools. This backbone-agnostic behavior follows from AGENTWM’s design: watermarks are defined over action-sequence distributions (Sec. 4.1), not model-specific embeddings, making them invariant to the underlying architecture. In practice, providers can swap backbone LLMs without re-engineering the watermarking pipeline.

Impact of Cross-model Imitation. Prior experiments assume both victim and attacker share the same backbone LLM. In practice, adversaries may fine-tune a different public model (Sec. 3.1). We evaluate this scenario by building \mathcal{M}_{vic} on Minstral-8B or Qwen3-8B, while \mathcal{M}_{imi} uses Qwen3-4B fine-tuned on stolen trajectories. As shown in Table 12, cross-model imitation remains effective. When the victim uses Minstral-8B, the Qwen3-4B-based \mathcal{M}_{imi} achieves a PR of 0.661 versus the victim’s 0.702. Despite differing architectures and fewer parameters, \mathcal{M}_{imi} closely replicates the victim’s capabilities, confirming that imitation threats extend beyond same-backbone scenarios.

Impact of δ on Watermark Strength. As mentioned in Sec. 4.2, δ controls the bias strength in our target distribution derivation. To understand how δ affects both watermark detectability and trajectory quality, we evaluate six δ values ranging from 0 (no watermark) to 5 (maximum strength). We measure two key metrics: Kullback-Leibler Divergence (KLD) quantifies how much the watermarked distribution \hat{D}_i deviates from the natural distribution

TABLE 12
Cross-model imitation performance.

Model	PR	RS	TS
\mathcal{M}_{vic} (Minstral-8B)	0.702	0.582	0.904
\mathcal{M}_{imi} (Qwen3-4B)	0.661	0.562	0.858
\mathcal{M}_{vic} (Qwen3-8B)	0.742	0.586	0.910
\mathcal{M}_{imi} (Qwen3-4B)	0.689	0.565	0.873

TABLE 13
Impact of watermark strength (δ).

Watermark Strength (δ)	0	1	2	3	4	5
KLD	—	0.096	0.386	0.801	1.408	1.808
TS	0.727	0.712	0.712	0.707	0.694	0.671

D_i , while TS assesses the quality of watermarked action sequences using LLM-as-a-judge evaluation. As shown in Table 13, increasing δ creates a trade-off between watermark strength and trajectory quality. KLD grows exponentially from 0.096 ($\delta = 1$) to 1.808 ($\delta = 5$), indicating progressively stronger distribution shifts. Concurrently, TS degrades from 0.712 to 0.671, revealing that excessive bias introduces semantic drift in action sequences. This trend exposes a critical vulnerability: overly aggressive watermarking not only compromises functional quality but also increases statistical detectability, potentially alerting sophisticated adversaries to the presence of embedded signatures. Based on these results, we recommend moderate δ values (2–3) for practical deployment. This range achieves sufficient watermark detectability while maintaining high trajectory fidelity, balancing IP protection with service quality.

8 CONCLUSION

In this work, we uncover the susceptibility of commercial agentic systems to imitation attacks and propose AGENTWM, the first watermarking framework designed for grey-box agentic models. By exploiting semantic equivalence in action spaces, AGENTWM injects imperceptible yet verifiable signatures into execution trajectories without compromising service quality. Extensive evaluations across diverse domains demonstrate that AGENTWM achieves near-perfect detection and user attribution accuracy while maintaining strong robustness against sophisticated removal attempts. As agentic AI evolves, AGENTWM provides a foundational and practical safeguard for protecting proprietary model capabilities in the wild.

REFERENCES

- [1] Z. Xi, W. Chen, X. Guo, W. He, Y. Ding, B. Hong, M. Zhang, J. Wang, S. Jin, E. Zhou *et al.*, “The rise and potential of large language model based agents: A survey,” *Science China Information Sciences*, vol. 68, no. 2, p. 121101, 2025.
- [2] L. Wang, C. Ma, X. Feng, Z. Zhang, H. Yang, J. Zhang, Z. Chen, J. Tang, X. Chen, Y. Lin *et al.*, “A survey on large language model based autonomous agents,” *Frontiers of Computer Science*, vol. 18, no. 6, p. 186345, 2024.
- [3] S. Yao, J. Zhao, D. Yu, N. Du, I. Shafran, K. R. Narasimhan, and Y. Cao, “React: Synergizing reasoning and acting in language models,” in *The eleventh international conference on learning representations*, 2022.
- [4] D. Hendrycks, C. Burns, S. Basart, A. Zou, M. Mazeika, D. Song, and J. Steinhardt, “Measuring massive multitask

language understanding,” in *International Conference on Learning Representations*.

[5] K. Valmeekam, A. Olmo, S. Sreedharan, and S. Kambhampati, “Large language models still can’t plan (a benchmark for llms on planning and reasoning about change),” in *NeurIPS 2022 Foundation Models for Decision Making Workshop*, 2022.

[6] A. Patel, C. Raffel, and C. Callison-Burch, “Datadreamer: A tool for synthetic data generation and reproducible llm workflows,” *arXiv preprint arXiv:2402.10379*, 2024.

[7] S. Hong, Y. Lin, B. Liu, B. Liu, B. Wu, C. Zhang, D. Li, J. Chen, J. Zhang, J. Wang *et al.*, “Data interpreter: An llm agent for data science,” in *Findings of the Association for Computational Linguistics: ACL 2025*, 2025, pp. 19 796–19 821.

[8] J. Wang, R. Jiang, C. Yang, Z. Wu, M. Onizuka, R. Shibasaki, N. Koshizuka, and C. Xiao, “Large language models as urban residents: An llm agent framework for personal mobility generation,” *Advances in Neural Information Processing Systems*, vol. 37, pp. 124 547–124 574, 2024.

[9] M. Z. Pan, M. Cemri, L. A. Agrawal, S. Yang, B. Chopra, R. Tiwari, K. Keutzer, A. Parameswaran, K. Ramchandran, D. Klein *et al.*, “Why do multiagent systems fail?” in *ICLR 2025 Workshop on Building Trust in Language Models and Applications*, 2025.

[10] OpenAI, “Openai o3 system card,” 2025. [Online]. Available: <https://openai.com/index/introducing-o3-and-o4-mini/>

[11] D. Guo, D. Yang, H. Zhang, J. Song, R. Zhang, R. Xu, Q. Zhu, S. Ma, P. Wang, X. Bi *et al.*, “Deepseek-r1: Incentivizing reasoning capability in llms via reinforcement learning,” *arXiv preprint arXiv:2501.12948*, 2025.

[12] Minimax, “Minimax 2.1 system card,” 2025. [Online]. Available: <https://www.minimax.io/news/minimax-m21>

[13] K. Zhao, L. Li, K. Ding, N. Z. Gong, Y. Zhao, and Y. Dong, “A survey on model extraction attacks and defenses for large language models,” in *Proceedings of the 31st ACM SIGKDD Conference on Knowledge Discovery and Data Mining V. 2*, 2025, pp. 6227–6236.

[14] Y. Liu, Y. Jia, J. Jia, and N. Z. Gong, “Evaluating {LLM-based} personal information extraction and countermeasures,” in *34th USENIX Security Symposium (USENIX Security 25)*, 2025, pp. 1669–1688.

[15] N. Carlini, D. Paleka, K. Dvijotham, T. Steinke, J. Hayase, A. F. Cooper, K. Lee, M. Jagielski, M. Nasr, A. Conmy *et al.*, “Stealing part of a production language model,” in *Proceedings of the 41st International Conference on Machine Learning*, 2024, pp. 5680–5705.

[16] Z. Li, D. Wu, S. Wang, and Z. Su, “Differentiation-based extraction of proprietary data from fine-tuned llms,” in *Proceedings of the 2025 ACM SIGSAC Conference on Computer and Communications Security*, 2025, pp. 3071–3085.

[17] A. Zou, Z. Wang, N. Carlini, M. Nasr, J. Z. Kolter, and M. Fredrikson, “Universal and transferable adversarial attacks on aligned language models,” *arXiv preprint arXiv:2307.15043*, 2023.

[18] S. Yi, Y. Liu, Z. Sun, T. Cong, X. He, J. Song, K. Xu, and Q. Li, “Jailbreak attacks and defenses against large language models: A survey,” *arXiv preprint arXiv:2407.04295*, 2024.

[19] I. Goodfellow, P. McDaniel, and N. Papernot, “Making machine learning robust against adversarial inputs,” *Communications of the ACM*, vol. 61, no. 7, pp. 56–66, 2018.

[20] I. J. Goodfellow, J. Shlens, and C. Szegedy, “Explaining and harnessing adversarial examples,” *arXiv preprint arXiv:1412.6572*, 2014.

[21] Z. Li, C. Wang, S. Wang, and C. Gao, “Protecting intellectual property of large language model-based code generation apis via watermarks,” in *Proceedings of the 2023 ACM SIGSAC Conference on Computer and Communications Security*, 2023, pp. 2336–2350.

[22] X. He, Q. Xu, Y. Zeng, L. Lyu, F. Wu, J. Li, and R. Jia, “Cater: Intellectual property protection on text generation apis via conditional watermarks,” *Advances in Neural Information Processing Systems*, vol. 35, pp. 5431–5445, 2022.

[23] R. Zhang, S. S. Hussain, P. Neekhara, and F. Koushanfar, “{REMARK-LLM}: A robust and efficient watermarking framework for generative large language models,” in *33rd USENIX Security Symposium (USENIX Security 24)*, 2024, pp. 1813–1830.

[24] Z. Zhao, X. Liu, S. Jha, P. McDaniel, B. Li, and C. Xiao, “Can watermarks be used to detect llm ip infringement for free?” in *The Thirteenth International Conference on Learning Representations*, 2025.

[25] S. Dathathri, A. See, S. Ghaisas, P.-S. Huang, R. McAdam, J. Welbl, V. Bachani, A. Kaskasoli, R. Stanforth, T. Matejovicova, J. Hayes, N. Vyas, M. A. Merey, J. Brown-Cohen, R. Bunel, B. Balle, T. Cemgil, Z. Ahmed, K. Stacpoole, I. Shumailov, C. Baetu, S. Gowal, D. Hassabis, and P. Kohli, “Scalable watermarking for identifying large language model outputs,” *Nature*. [Online]. Available: <https://doi.org/10.1038/s41586-024-08025-4>

[26] G. Alon and M. Kamfonas, “Detecting language model attacks with perplexity,” *arXiv preprint arXiv:2308.14132*, 2023.

[27] T. Brown, B. Mann, N. Ryder, M. Subbiah, J. D. Kaplan, P. Dhariwal, A. Neelakantan, P. Shyam, G. Sastry, A. Askell *et al.*, “Language models are few-shot learners,” *Advances in neural information processing systems*, vol. 33, pp. 1877–1901, 2020.

[28] H. W. Chung, L. Hou, S. Longpre, B. Zoph, Y. Tay, W. Fedus, Y. Li, X. Wang, M. Dehghani, S. Brahma *et al.*, “Scaling instruction-finetuned language models,” *Journal of Machine Learning Research*, vol. 25, no. 70, pp. 1–53, 2024.

[29] L. Ouyang, J. Wu, X. Jiang, D. Almeida, C. Wainwright, P. Mishkin, C. Zhang, S. Agarwal, K. Slama, A. Ray *et al.*, “Training language models to follow instructions with human feedback,” *Advances in neural information processing systems*, vol. 35, pp. 27 730–27 744, 2022.

[30] J. Schulman, F. Wolski, P. Dhariwal, A. Radford, and O. Klimov, “Proximal policy optimization algorithms,” *arXiv preprint arXiv:1707.06347*, 2017.

[31] C. Zhou, P. Liu, P. Xu, S. Iyer, J. Sun, Y. Mao, X. Ma, A. Efrat, P. Yu, L. Yu *et al.*, “Lima: Less is more for alignment,” *Advances in Neural Information Processing Systems*, vol. 36, pp. 55 006–55 021, 2023.

[32] Y. Ye, Z. Huang, Y. Xiao, E. Chern, S. Xia, and P. Liu, “Limo: Less is more for reasoning,” *arXiv preprint arXiv:2502.03387*, 2025.

[33] “Coze platform.” [Online]. Available: <https://www.coze.com/>

[34] “Dify platform.” [Online]. Available: <https://dify.ai/>

[35] Z. Li, J. Cui, X. Liao, and L. Xing, “Les dissonances: Cross-tool harvesting and polluting in multi-tool empowered llm agents,” *NDSS 2026*.

[36] L. Wang, W. Wang, S. Wang, Z. Li, Z. Ji, Z. Lyu, D. Wu, and S.-C. Cheung, “Ip leakage attacks targeting llm-based multi-agent systems,” *arXiv preprint arXiv:2505.12442*, 2025.

[37] X. Li, T. Qiu, Y. Jin, L. Wang, H. Guo, X. Jia, X. Wang, and W. Dong, “Webcloak: Characterizing and mitigating the threats of llm-driven web agents as intelligent scrapers,” in *IEEE Symposium on Security and Privacy*, 2026.

[38] Y. Ji, Z. Ma, Y. Wang, G. Chen, X. Chu, and L. Wu, “Tree search for llm agent reinforcement learning,” *arXiv preprint arXiv:2509.21240*, 2025.

[39] W. Chen, J. Yuan, C. Qian, C. Yang, Z. Liu, and M. Sun, “Optima: Optimizing effectiveness and efficiency for llm-based multi-agent system,” in *Findings of the Association for Computational Linguistics: ACL 2025*, 2025, pp. 11534–11557.

[40] Y. Zhai, T. Yang, K. Xu, D. Feng, C. Yang, B. Ding, and H. Wang, “Enhancing decision-making for llm agents via step-level q-value models,” in *Proceedings of the AAAI Conference on Artificial Intelligence*.

[41] J. Y. Koh, S. McAleer, D. Fried, and R. Salakhutdinov, “Tree search for language model agents,” *arXiv preprint arXiv:2407.01476*, 2024.

[42] N. Carlini, J. Hayes, M. Nasr, M. Jagielski, V. Sehwag, F. Tramer, B. Balle, D. Ippolito, and E. Wallace, “Extracting training data from diffusion models,” in *32nd USENIX security symposium (USENIX Security 23)*, 2023, pp. 5253–5270.

[43] J. Kirchenbauer, J. Geiping, Y. Wen, J. Katz, I. Miers, and T. Goldstein, “A watermark for large language models,” in *International Conference on Machine Learning*. PMLR, 2023, pp. 17061–17084.

[44] Y. Liu and Y. Bu, “Adaptive text watermark for large language models,” in *Proceedings of the 41st International Conference on Machine Learning*, 2024, pp. 30718–30737.

[45] A. Liu, L. Pan, X. Hu, S. Meng, and L. Wen, “A semantic invariant robust watermark for large language models,” in *The Twelfth International Conference on Learning Representations*.

[46] A. Hou, J. Zhang, T. He, Y. Wang, Y.-S. Chuang, H. Wang, L. Shen, B. Van Durme, D. Khashabi, and Y. Tsvetkov, “Semstamp: A semantic watermark with paraphrastic robustness for text generation,” in *NAACL*, 2024, pp. 4067–4082.

[47] J. Fu, X. Zhao, R. Yang, Y. Zhang, J. Chen, and Y. Xiao, “Gumbelsoft: Diversified language model watermarking via the gumbelmax-trick,” in *ACL*.

[48] Y. Wen, J. Guo, and H. Huang, “Cotguard: Using chain-of-thought triggering for copyright protection in multi-agent llm systems,” *arXiv preprint arXiv:2505.19405*, 2025.

[49] K. Huang, Z. Zhang, Z. Yang, and L. Zhou, “Agent guide: A simple agent behavioral watermarking framework,” *arXiv preprint arXiv:2504.05871*, 2025.

[50] D.-h. Yoon, M. Chun, T. Allen, H. Müller, M. Wang, and R. Sharma, “Intrinsic fingerprint of llms: Continue training is not all you need to steal a model!” *arXiv preprint arXiv:2507.03014*, 2025.

[51] S. Shao, Y. Li, H. Yao, Y. He, Z. Qin, and K. Ren, “Explanation as a watermark: Towards harmless and multi-bit model ownership verification via watermarking feature attribution,” *arXiv preprint arXiv:2405.04825*, 2024.

[52] J. Xu, F. Wang, M. Ma, P. W. Koh, C. Xiao, and M. Chen, “Instructional fingerprinting of large language models,” in *Proceedings of the 2024 Conference of the North American Chapter of the Association for Computational Linguistics: Human Language Technologies (Volume 1: Long Papers)*, 2024, pp. 3277–3306.

[53] X. Shen, Y. Wang, X. Shi, Y. Wang, P. Zhao, and J. Gu, “Efficient reasoning with hidden thinking,” *arXiv preprint arXiv:2501.19201*, 2025.

[54] Y. Yang, C. Li, Q. Li, O. Ma, H. Wang, Z. Wang, Y. Gao, W. Chen, and S. Ji, “PRSA: Prompt stealing attacks against Real-World prompt services,” in *34th USENIX security symposium (USENIX Security 25)*, 2025, pp. 2283–2302.

[55] N. Carlini, F. Tramèr, E. Wallace, M. Jagielski, A. Herbert-Voss, K. Lee, A. Roberts, T. Brown, D. Song, Ú. Erlingsson, A. Oprea, and C. Raffel, “Extracting training data from large language models,” in *30th USENIX Security Symposium (USENIX Security 21)*.

[56] A. Yang, A. Li, B. Yang, B. Zhang, B. Hui, B. Zheng, B. Yu, C. Gao, C. Huang, C. Lv *et al.*, “Qwen3 technical report,” *arXiv preprint arXiv:2505.09388*, 2025.

[57] V. Chandrasekaran, K. Chaudhuri, I. Giacomelli, S. Jha, and S. Yan, “Exploring connections between active learning and model extraction,” in *29th USENIX Security Symposium (USENIX Security 20)*, 2020, pp. 1309–1326.

[58] “Manus platform.” [Online]. Available: <https://www.manus.ai/>

[59] H. Gilbert and H. Handschuh, “Security analysis of sha-256 and sisters,” in *International workshop on selected areas in cryptography*. Springer, 2003, pp. 175–193.

[60] Z. Liu, T. Hoang, J. Zhang, M. Zhu, T. Lan, J. Tan, W. Yao, Z. Liu, Y. Feng, R. RN *et al.*, “Apigen: Automated pipeline for generating verifiable and diverse function-calling datasets,” *Advances in Neural Information Processing Systems*, vol. 37, pp. 54463–54482, 2024.

[61] “Qwen3-embedding-0.6b.” [Online]. Available: <https://huggingface.co/Qwen/Qwen3-Embedding-0.6B>

[62] OpenAI, “Gpt-5 system card,” 2025. [Online]. Available: <https://openai.com/index/gpt-5-system-card/>

[63] A. Liu, A. Mei, B. Lin, B. Xue, B. Wang, B. Xu, B. Wu, B. Zhang, C. Lin, C. Dong *et al.*, “Deepseek-v3. 2: Pushing the frontier of open large language models,” *arXiv preprint arXiv:2512.02556*, 2025.

[64] S. Yao, N. Shinn, P. Razavi, and K. Narasimhan, “ τ -bench: A Benchmark for Tool-Agent-User Interaction in Real-World Domains,” *ICLR 2025*, 2024.

[65] Y. Qin, S. Liang, Y. Ye, K. Zhu, L. Yan, Y. Lu, Y. Lin, X. Cong, X. Tang, B. Qian *et al.*, “Toolllm: Facilitating large language models to master 16000+ real-world apis,” in *The Twelfth International Conference on Learning Representations*.

[66] M. Chang, J. Zhang, Z. Zhu, C. Yang, Y. Yang, Y. Jin, Z. Lan, L. Kong, and J. He, “Agentboard: An analytical evaluation board of multi-turn llm agents,” *Advances in neural information processing systems*, vol. 37, pp. 74325–74362, 2024.

[67] M. Zhuge, C. Zhao, D. R. Ashley, W. Wang, D. Khizbulin, Y. Xiong, Z. Liu, E. Chang, R. Krishnamoorthi, Y. Tian *et al.*, “Agent-as-a-judge: Evaluate agents with agents,” in *ICML 2024*.

[68] P. Clark, I. Cowhey, O. Etzioni, T. Khot, A. Sabharwal, C. Schoenick, and O. Tafjord, “Think you have solved question answering? try arc, the ai2 reasoning challenge,” *arXiv preprint arXiv:1803.05457*, 2018.

[69] H. Kokel, M. Katz, K. Srinivas, and S. Sohrabi, “Acpbench: Reasoning about action, change, and planning,” in *Proceedings of the AAAI Conference on Artificial Intelligence*, vol. 39, no. 25, 2025, pp. 26 559–26 568.

[70] M. Kang, J. Jeong, S. Lee, J. Cho, and S. J. Hwang, “Distilling llm agent into small models with retrieval and code tools,” *arXiv preprint arXiv:2505.17612*, 2025.

[71] “Minstral-8b-instruct-2410.” [Online]. Available: <https://huggingface.co/mistralai/Minstral-8B-Instruct-2410>

[72] “Qwen3-next-80b-a3b.” [Online]. Available: <https://huggingface.co/collections/Qwen/qwen3-next>

[73] E. J. Hu, Y. Shen, P. Wallis, Z. Allen-Zhu, Y. Li, S. Wang, L. Wang, W. Chen *et al.*, “Lora: Low-rank adaptation of large language models.” *ICLR*, vol. 1, no. 2, p. 3, 2022.

[74] R. Chen, Y. Wu, J. Guo, and H. Huang, “De-mark: Watermark removal in large language models,” in *Forty-second International Conference on Machine Learning*.

[75] L. Wang, W. Yang, D. Chen, H. Zhou, Y. Lin, F. Meng, J. Zhou, and X. Sun, “Towards codable watermarking for injecting multi-bits information to llms,” in *The Twelfth International Conference on Learning Representations*.

[76] A. Radford, J. Wu, R. Child, D. Luan, D. Amodei, I. Sutskever *et al.*, “Language models are unsupervised multitask learners,” *OpenAI blog*, vol. 1, no. 8, p. 9, 2019.

APPENDIX

To empirically validate the prevalence of grey-box visibility constraints in commercial agentic systems, we conducted a comprehensive survey of 29 mainstream agentic platforms and frameworks. We categorize each platform based on its default observability characteristics into three visibility levels:

- **White-box:** Systems that expose complete, token-level trajectory of LLM reasoning, including full input/output logs, intermediate chain-of-thought, and fine-grained execution details. These platforms typically support streaming tokens and comprehensive tracing infrastructure.
- **Grey-box:** Systems that reveal action sequences and summarized reasoning steps for billing and debugging purposes, but conceal raw token-level internal reasoning traces. This represents the dominant deployment model for commercial agentic services.
- **Black-box:** Systems that only expose final outputs with minimal visibility into intermediate execution steps or tool invocations.

Table 14 presents our classification results. We observe that 24 out of 29 platforms (82.8%) adopt the grey-box model, confirming our threat model assumption in Sec. 3.1. This visibility constraint fundamentally motivates AGENTWM’s design: existing watermarking techniques that rely on embedding signals into complete reasoning traces fail under grey-box constraints, necessitating our action-sequence-based approach.

TABLE 14
Classification of 29 mainstream agentic platforms by visibility level.
Platforms are categorized based on their default observability characteristics without additional third-party instrumentation.

Visibility	Count	Platforms Name
White-box	3	LangGraph, Langfuse, PydanticAI
Grey-box	24	Coze, Dify.ai, CrewAI, Semantic Kernel, Microsoft Copilot Studio, Salesforce Agentforce, Google Vertex AI, Relevance AI, Dust, Llyz, Cognosys, Glean Agents, Taskade, Make.com, Vellum AI, Genspark Super Agent, Manus AI, LangFlow, Boomi AI Studio, Sierra, n8n, Fiddler AI, Microsoft Agent Framework, Google Gemini
Black-box	2	Devin, Workday Illuminate